

# Viscoelastic twist properties of some nematic liquid crystalline azoxybenzenes

J. W. van Dijk, W. W. Beens, and W. H. de Jeu

*Solid State Physics Laboratory, 1 Melkweg, 9718 EP Groningen, The Netherlands*  
(Received 26 May 1983; accepted 30 June 1983)

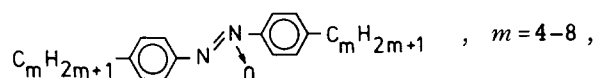
The static and dynamic behavior of the Frederiks transition for twist of a uniform planar nematic sample in an external magnetic field has been studied by monitoring the associated conoscopic figure. In particular, the decay of this figure after the field has been switched off is considered in detail in order to obtain results for the twist viscosity  $\gamma_1$ . Results for the twist elastic constant  $K_2$  and for the viscosity  $\gamma_1$  are reported for the homologous series of *p, p'*-dialkylazoxybenzenes.  $K_2$  is found to be smaller than both  $K_1$  and  $K_3$ , while  $K_2$  varies little along the series. The temperature dependence of  $\gamma_1$  can be described by a combination of an activated process and a term depending on the orientational order parameter.

## I. INTRODUCTION

Nematic liquid crystals are anisotropic liquids in which the constituting molecules are, on average, aligned with a certain axis parallel to a preferred direction in space, given by the director  $\mathbf{n}$ . In an actual sample, the orientation  $\mathbf{n}$  is determined by boundary conditions and external fields. Variations of  $\mathbf{n}$  in space and time, respectively, can be described by a continuum theory.<sup>1</sup> The elastic properties are governed by three curvature elastic constants, corresponding to the restoring torques opposing splays ( $K_1$ ), twists ( $K_2$ ), and bends ( $K_3$ ). The hydrodynamic properties are determined by five independent viscosity coefficients. Two of these are related to reorientation of the director, without material flow being involved. Apart from the inherent interest in these properties (e.g., the elastic constants are related to the gradients of the intermolecular interactions), they are of great importance for the performance of materials in liquid crystal displays.

Measurements of the elastic constants are relatively numerous,<sup>2</sup> and are usually performed by determining the threshold for deformation of a uniform director pattern in an external field (Frederiks transition). The attention has been focused mainly on  $K_1$  and  $K_3$ . Much fewer results are available for  $K_2$ ,<sup>3</sup> probably because the deformation of the director pattern is not so easily observed in the relevant twist geometry as in the cases of  $K_1$  and  $K_3$ . Alternatively,  $K_{\text{eff}} = K_1 + \frac{1}{4}K_3 - \frac{1}{2}K_2$  has been determined from the deformation of a planar nematic layer twisted over an angle of  $\pi/2$  in an external magnetic field. If  $K_1$  and  $K_3$  are known, then  $K_2$  can also be obtained, though much less accurately.<sup>2</sup> Full information on the viscosity coefficients is only available for very few compounds.<sup>4</sup> For practical reasons, attention has been given mainly to the shear-alignment viscosity<sup>5</sup>  $\eta_s$  and to the viscosity  $\gamma_1$ .<sup>6</sup> The latter quantity is important for switching times of liquid crystal displays. To determine  $\gamma_1$  frequently rotating field methods<sup>2</sup> are used, which unfortunately require a relatively large amount of material.

In this paper, we give results for  $K_2$  and  $\gamma_1$  of the homologous series of *p, p'*-dialkylazoxybenzenes



to be indicated as *mAB*.  $K_2$  is obtained from the Frederiks transition for twist of a uniform planar sample in an external magnetic field. The threshold field  $H_c$  is found from the rotation angle  $\delta$  of the associated conoscopic figure, as originally proposed by Cladis<sup>7</sup> and developed further by Leenhouts.<sup>8</sup> Furthermore,  $\gamma_1$  is obtained from the dynamics of the same Frederiks transition. The precision with which  $\delta(t)$  can be measured at small angles, and thus the feasibility of the whole method, has been greatly improved by photographing the cone-scope figure at fixed time intervals, and measuring  $\delta$  from the resulting negatives.  $K_2$  increases only slightly along the *mAB* series, with pronounced alternation with *m* in a fashion similar to that observed for  $K_1$  and  $K_3$ . The temperature variation of  $\gamma_1$  is governed by an activated process on which the dependence of the orientational order parameter is superimposed.

## II. EXPERIMENTAL

When a magnetic field  $H$  is applied to a uniform planar nematic layer ( $\mathbf{n}$  parallel to one direction in the plane of the substrate) such that  $H$  is parallel to the layer and perpendicular to  $\mathbf{n}$ , distortion of  $\mathbf{n}$  starts at the threshold field given by<sup>1,2</sup>

$$H_c = (\pi/d)(K_2/\Delta\chi)^{1/2}. \quad (1)$$

Here,  $d$  is the thickness of the layer and  $\Delta\chi$  the anisotropy of the magnetic susceptibility. Above  $H_c$  the maximum twist angle  $\phi_m$  in the middle of the sample is determined by the relation

$$H/H_c = (2/\pi)F(\frac{1}{2}\pi, \phi_m), \quad (2)$$

where  $F$  is the complete elliptic integral of the first kind. The conoscopic figure associated with a uniform planar nematic layer consists of two hyperbola. When a twist deformation is applied, this pattern is rotated over an angle  $\delta$  given by<sup>7</sup>

$$\begin{aligned} \tan 2\delta &= \langle \sin 2\phi(z) \rangle / \langle \cos 2\phi(z) \rangle \\ &= 2 \sin \phi_m / [2E(\frac{1}{2}\pi, \sin \phi_m) - F(\frac{1}{2}\pi, \sin \phi_m)]. \end{aligned} \quad (3)$$

Here  $\phi(z)$  is the twist angle of  $\mathbf{n}$ , and  $z = \pm \frac{1}{2}d$  defines the boundaries of the nematic layer where strong anchoring ( $\phi = 0$ ) is assumed. In Eq. (3), the brackets denote an average, while  $E$  is the complete elliptic integral of the second kind. For  $H \gg H_c$  one finds that  $\phi_m \rightarrow \frac{1}{2}\pi$  and also  $\delta \rightarrow \frac{1}{2}\pi$ . As discussed by Leenhouts,<sup>8</sup> if  $\mathbf{H}$  is perpendicular to  $\mathbf{n}$ , the conoscopic pattern can rotate either clockwise or counterclockwise. In practice, both of these will occur simultaneously in different regions of the sample, which makes an accurate determination of  $\delta$  impossible. This problem can be overcome by orienting  $\mathbf{H}$  at an angle of  $(90^\circ - \phi_0)$  to  $\mathbf{n}$ . In this case, the deformation already starts at  $H=0$ , and Eqs. (2) and (3) have to be replaced by<sup>8</sup>

$$H/H_c = (2/\pi) \int_0^{\pi/2} d\psi (1 - \sin^2 \phi_m \sin^2 \psi)^{-1/2}, \quad (4)$$

$$\tan 2\delta = \frac{2(\sin^2 \phi_m - \sin^2 \phi_0)^{1/2} \cos 2\phi_0 - H(\psi_0, \phi_m) \sin 2\phi_0}{2(\sin^2 \phi_m - \sin^2 \phi_0)^{1/2} \sin 2\phi_0 + H(\psi_0, \phi_m) \cos 2\phi_0}. \quad (5)$$

Here  $\sin \psi_0 = \sin \phi_0 / \sin \phi_m$  and  $H(\psi_0, \phi_m)$  is given by

$$H(\psi_0, \phi_m) = 2 \int_0^{\pi/2} d\psi (1 - \sin^2 \phi_m \sin^2 \psi)^{1/2} \times \int_0^{\pi/2} d\psi (1 - \sin^2 \phi_m \sin^2 \psi). \quad (6)$$

In practice  $\phi_0$  is restricted to a few degrees and is only known within approximately one degree. The angle  $\delta$  is recorded as a function of  $H$ . By making a nonlinear least-square fit to Eqs. (4) and (5), values for  $H_c$  and  $\phi_0$  are obtained. With Eq. (1),  $H_c$  leads finally to values for  $K_2$ , while the constancy of  $\phi_0$  with temperature gives an indication of the quality of the fitting procedure.

If a field  $H > H_c$  is switched on, the dynamic equation for  $\phi(z, t)$  is given by<sup>9</sup>

$$K_2 \partial^2 \phi / \partial z^2 + \sin \phi \cos \phi \Delta \chi H^2 = \gamma_1 \partial \phi / \partial t. \quad (7)$$

The general solution for  $\phi(z, t)$  can be expressed as a power series

$$\phi(z, t) = \sum_n C_n(t) \cos[(2n+1)\pi z/d]. \quad (8)$$

Equating the left-hand side of Eq. (7) to zero gives the equilibrium values for  $\phi(z)$ . If the field is now

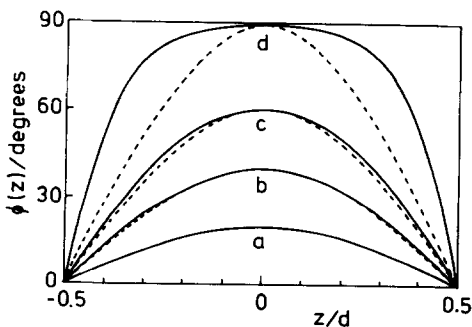


FIG. 1. Twist angle  $\phi(z)$  for values of  $\phi_m$  of  $20^\circ$ ,  $40^\circ$ ,  $60^\circ$ , and  $89^\circ$ , respectively (a, b, c, d). Full lines: complete theory, broken lines: approximation of Eq. (11).

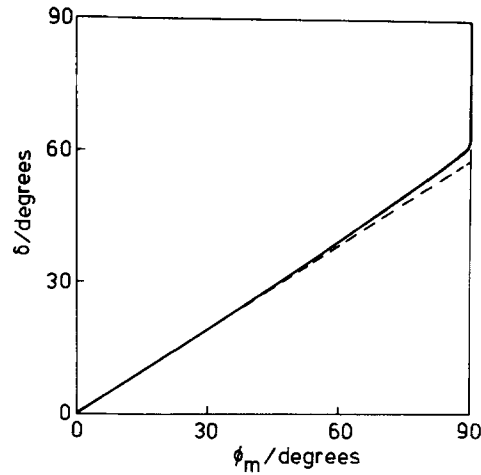


FIG. 2. Rotation angle  $\delta$  of the conoscopic figure vs  $\phi_m$ : full and broken lines as in Fig. 1.

switched off, the eigenfunctions of  $\phi(z, t)$  decay with characteristic time constants

$$\tau_n^{-1} = (K_2/\gamma_1) [(2n+1)\pi/d]^2. \quad (9)$$

The time constant  $\tau_0$  gives the slowest decay corresponding to the least distorted solution. Provided  $\phi_m(0)$  is not too large, one expects a simple exponential decay

$$\phi(z, t) = \phi(z, 0) \exp(-t/\tau_0), \quad (10)$$

with

$$\phi(z, 0) = \phi_m \cos(\pi z/d) \quad (11)$$

and

$$\tau_0 = \gamma_1 d^2 / (\pi^2 K_2) = \gamma_1 / (\Delta \chi H_c^2). \quad (12)$$

In Fig. 1, the full solution (8) is compared with the approximation (11). Experimentally, we measure the rotation angle  $\delta(t)$  of the conoscopic figure instead of  $\phi(z, t)$ . The relation between  $\delta$  and  $\phi_m$  is shown in Fig. 2, again for the approximation (11) and the full solution. From these results, we conclude that for  $\phi_m \lesssim 40^\circ$  it is sufficient to do a simple measurement of  $\tau_0$  on  $\delta(t)$ , which then gives in turn  $\gamma_1$ .

The *mAB* compounds were synthesized at the Philips Research Laboratories (Eindhoven) as described in Ref. 10. The transition temperatures [nematic-isotropic (NI)] are given in Table I. Uniform planar samples were made by using two glass plates coated with para-xylylene,<sup>11</sup> first rubbed gently in one direction. The glass plates were kept apart by tungsten ribbon of 100  $\mu\text{m}$  thickness. The exact thickness, determined by interferometry on the empty cell, was usually somewhat higher.

The conosccope used has been described in Ref. 8. Conoscope and oven with sample are both placed in the gap of a Bruker BE15 electromagnet that provides a maximum field of 1.1 T over 50 mm. By means of crosswires mounted in the focal plane of the ocular, the rotation angle  $\delta$  of the conoscopic pattern can be determined using a graduated scale attached to the ocular tube. The oven with glass windows is contained in a copper jacket. Using a PID controller (Eurotherm 093)

TABLE I. Values of  $K_2$  and  $\gamma_1$  of the  $mAB$  series.

$m=4$			$m=5$			$m=6$		
$t/^\circ\text{C}$	$K_2/10^{-12}\text{ N}$	$\gamma_1/10^{-3}\text{ Pa s}$	$t/^\circ\text{C}$	$K_2/10^{-12}\text{ N}$	$\gamma_1/10^{-3}\text{ Pa s}$	$t/^\circ\text{C}$	$K_2/10^{-12}\text{ N}$	$\gamma_1/10^{-3}\text{ Pa s}$
20.2	2.79	...	30.1	7.77	94.8	30.1	4.83	78.3
21.2	...	64.2	39.8	6.60	68.9	35.4	4.17	61.7
23.4	2.54	55.0	45.3	5.91	55.2	39.8	3.71	52.8
25.4	2.29	45.7	49.6	5.27	42.3	45.3	2.71	33.1
26.5	...	42.7	55.2	4.58	34.4	47.5	2.41	...
27.7	1.97	33.6	59.4	3.82	25.6	48.7	2.19	25.6
28.8	1.62	29.5	61.8	3.40	21.7	49.6	2.04	23.5
30.9	NI	...	64.0	2.81	16.8	50.8	1.84	21.2
			65.0	2.44	16.3	52.0	1.47	18.7
			66.0	1.94	13.3	53.2	NI	...
			66.6	NI	...			
$m=7$			$m=8$					
$t/^\circ\text{C}$	$K_2/10^{-12}\text{ N}$	$\gamma_1/10^{-3}\text{ Pa s}$	$t/^\circ\text{C}$	$K_2/10^{-12}\text{ N}$	$\gamma_1/10^{-3}\text{ Pa s}$			
54.2	7.11	54.3	64.0	3.79	38.8			
57.3	5.95	40.0	65.0	2.68	27.0			
59.4	5.37	38.4	66.2	NI	...			
61.8	4.62	...						
62.9	...	32.0						
64.0	4.05	...						
66.0	3.43	23.3						
67.1	3.07	18.3						
68.2	2.70	23.5						
69.4	2.03	16.0						
70.1	NI	...						

the temperature is kept constant within  $0.1^\circ\text{C}$ . To record the decay of  $\delta(t)$  after the field has been switched off, photographs were taken using a Wild MPS 51S automatic camera in combination with a homebuilt electronic timer. The minimum time interval between two exposures is determined by the motor drive of the film transport, and is about 1 s. Using a mercury light source with interference filter at 546 nm and high-speed film, exposure times as short as 0.01 s can be obtained.

### III. RESULTS

The results for both  $K_2$  and  $\gamma_1$  of the  $mAB$  series are given in Table I. Figure 3 shows a typical plot of the decay of  $\delta$  vs time when the field is switched off, starting at approximately  $\delta \approx 45^\circ$ . As one can see, the scat-

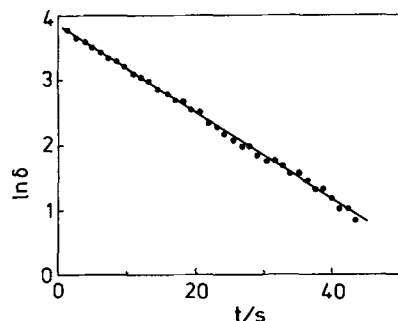


FIG. 3. Typical decay of the rotation angle  $\delta$  of the conoscopic figure.

ter of experimental points around the straight line increases at small values of  $\delta$ , due to increased relative error in the determination of  $\delta$ . Figure 4 shows plots of  $K_2$  vs the reduced temperature. In order to obtain  $K_2$  from  $H_c$ , data for the anisotropy of the magnetic susceptibility are required, which were taken from Ref. 12. For 4AB and 7AB, the values of  $K_2$  agree reasonably well with the less accurate values obtained earlier from the threshold of a twisted nematic layer.<sup>13</sup> For 5AB and 6AB, there are considerable differences. Finally, in Fig. 5, Arrhenius type plots of  $\ln \gamma_1$  vs  $1/T$  are shown. As we see, no straight lines are obtained, indicating a more complicated dependence on the temperature.

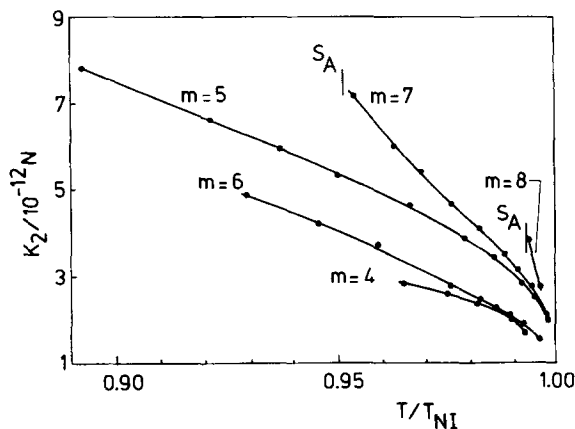


FIG. 4. Twist elastic constants  $K_2$  of the  $mAB$  series.

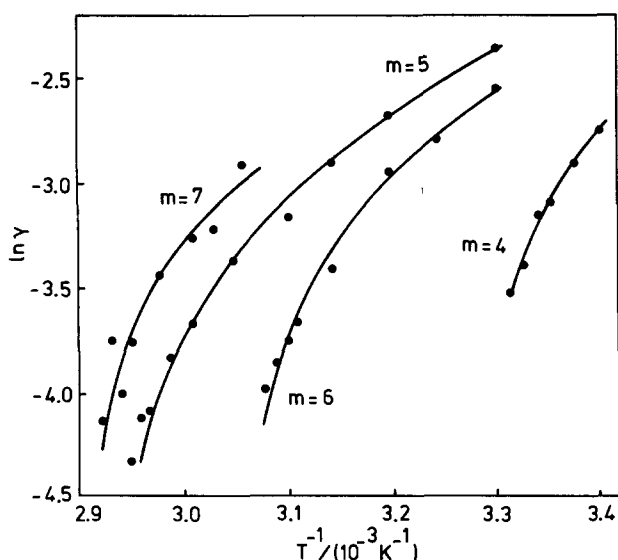


FIG. 5. Twist viscosity  $\gamma_1$  vs inverse temperature for the  $mAB$  series; full lines give least-square fits of the data to Eq. (14).

#### IV. DISCUSSION

From Fig. 4, we note that along the homologous series  $K_2$  increases somewhat, superimposed on a pronounced alternation with  $m$ . This behavior is compared for all three  $K_i$  in Fig. 6. Apart from the alternation, the variation of  $K_2$  is rather small. This is similar to the behavior in some other homologous series.<sup>3(e),8(b)</sup>

From a simple Landau theory of the NI transition, one obtains in the lowest-order approximation<sup>2</sup>

$$\begin{aligned} K_1 = K_3 &= 2S^2(L_1 + \frac{1}{2}L_2), \\ K_2 &= 2S^2L_1. \end{aligned} \quad (13)$$

Here  $S = \langle \frac{3}{2} \cos^2 \beta - \frac{1}{2} \rangle$  is the usual nematic order parameter, where  $\beta$  is the angle between the long molecular axis and the director, and  $L_1$  and  $L_2$  are coefficients in the second-order gradient terms in the Landau expansion in the order parameter. For the  $mAB$  series,  $S$  is known to be higher for the members with odd  $m$  compared to the even valued ones,<sup>12</sup> which explains the observed alternation of the  $K_i$ . As  $K_2$  is the smallest of the three constants, we conclude from Eq. (13) that  $L_2$

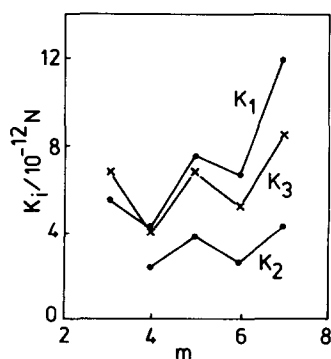


FIG. 6. Variation of the elastic constants with the chain length at  $T = 0.98 T_{NI}$ .

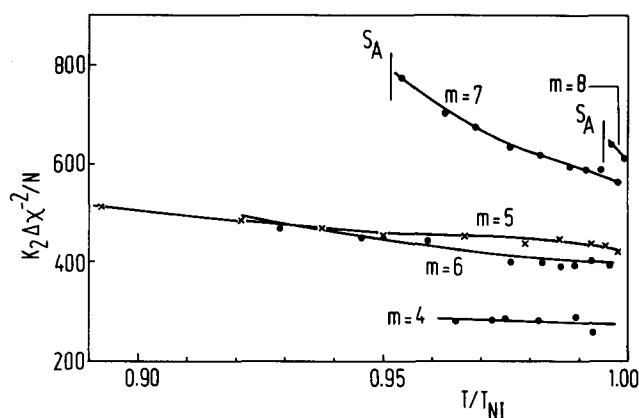


FIG. 7. Plot of  $K_2/\Delta\chi^2$  vs reduced temperature for the  $mAB$  series.

is positive. This seems to be a general result for various types of compounds. Using the relation  $\Delta\chi \sim S$ —which holds, provided the molecules can be treated as effectively cylindrically symmetric—the proportionality between  $K_i$  and  $S^2$  can be checked by considering  $K_i/\Delta\chi^2$ . This quantity is displayed in Fig. 7 for  $K_2$ . The proportionality holds especially well for  $m=4$  where  $K_1 \approx K_3$ . Evidently, in this case the lowest-order approximation given by Eq. (13) is fully adequate.

The results for  $\gamma_1$  of the  $mAB$  series (Fig. 5) do not show the simple exponential dependence on the inverse temperature often observed in an isotropic liquid. Evidently, some indirect dependence on  $T$  via the order parameter  $S(T)$  is involved. In the literature, various proposals have been given to account for the total thermal behavior of  $\gamma_1$ .<sup>14</sup> Our data can be fitted reasonably well to the formula proposed by Martins *et al.*<sup>14(a)</sup>

$$\gamma_1 = cS^2 \exp(ES/k_B T). \quad (14)$$

The full curves in Fig. 5 correspond to a least-square fit of Eq. (14) to the data, with  $S$  taken again from Ref. 12 and values of  $c$  and  $E$  as given in Table II. There has been some disagreement about the actual temperature dependence of  $\gamma_1$ . As a consequence of the relatively limited variation of  $S$  in combination with an activated process, it is difficult to exclude formulas other than Eq. (14). The exponential form of Eq. (14) does not allow a meaningful comparison of  $\gamma_1$  values at the same reduced temperature. Taking the (extrapolated) values of  $\gamma_1$  at a fixed absolute temperature not too close to the nematic–isotropic transition, it is clear that  $\gamma_1$  increases with increasing chain length  $m$ .

TABLE II. Values of the coefficients  $c$  and  $E$  in Eq. (14) for various members of the  $mAB$  series.

$m$	$c$	$E$ (eV)
4	0.025	0.087
5	0.017	0.097
6	0.037	0.078
7	0.045	0.060

In conclusion, the conoscopic method to monitor the Frederiks transition for twist has been used to complete the results of the elastic constants of the  $mAB$  series. In addition, it has been shown that the decay of the rotation of the conoscopic figure provides a convenient practical method to determine  $\gamma_1$  on small samples.

#### ACKNOWLEDGMENTS

This work forms part of the research program of the Stichting voor Fundamenteel Onderzoek der Materie (Foundation for Fundamental Research on Matter—FOM) and was made possible by financial support by the Nederlandse Organisatie voor Zuiver-Wetenschappelijk Onderzoek (Netherlands Organization for the Advancement of Pure Research—ZWO).

- <sup>1</sup>See, for example, P. G. de Gennes, *The Physics of Liquid Crystals* (Clarendon, Oxford, 1974).
- <sup>2</sup>See, for example, W. H. de Jeu, *Physical Properties of Liquid Crystalline Materials* (Gordon and Breach, New York, 1980).
- <sup>3</sup>(a) V. Tsvetkov, *Acta Physicochim. URSS* **6**, 865 (1937); (b) C. Williams and P. E. Cladis, *Solid State Commun.* **10**, 357 (1972); (c) N. V. Madhusudana, P. P. Karat, and S. Chandrasekhar, *Pramana, Suppl. No. 1*, p. 225 (1975); (d) F. Leenhouts, F van der Woude, and A. J. Dekker, *Phys. Lett. A* **58**, 242 (1976); (e) N. V. Madhusudana and R. Pratibha, *Mol. Cryst. Liq. Cryst.* **89**, 249 (1982).
- <sup>4</sup>(a) W. H. de Jeu, *Phys. Lett. A* **69**, 122 (1978); (b) H. Knepppe and F. Schneider, *Mol. Cryst. Liq. Cryst.* **65**, 23 (1981); (c) H. Knepppe, F. Schneider, and N. K. Sharma, *Ber. Bunsenges. Phys. Chem.* **85**, 784 (1981); (d) W. W. Beens and W. H. de Jeu, *J. Phys.* **44**, 129 (1983).
- <sup>5</sup>See, for example, J. Constant and E. P. Raynes, *Mol. Cryst. Liq. Cryst.* **62**, 115 (1980).
- <sup>6</sup>(a) Older results are summarized in: C. K. Yun, *Phys. Lett. A* **43**, 369 (1973); (b) J. Prost and H. Gasparoux, *ibid.* **36**, 245 (1971); (c) G. Heppe and F. Schneider, *Z. Naturforsch. Teil A* **27**, 976 (1972); (d) P. J. Flanders, *Mol. Cryst. Liq. Cryst.* **29**, 19 (1974); (e) A. C. Diogo and A. F. Martins, *ibid.* **66**, 133 (1981); (f) P. R. Gerber, *Appl. Phys. A* **26**, 139 (1981); (g) H. Knepppe, F. Schneider, and N. K. Sharma, *J. Chem. Phys.* **77**, 3203 (1982).
- <sup>7</sup>P. E. Cladis, *Phys. Rev. Lett.* **28**, 1629 (1972).
- <sup>8</sup>(a) F. Leenhouts, Ph.D. thesis, University of Groningen, 1979; (b) F. Leenhouts and A. J. Dekker, *J. Chem. Phys.* **74**, 1956 (1981).
- <sup>9</sup>P. Pieranski, F. Brochard, and E. Guyon, *J. Phys.* **34**, 35 (1973).
- <sup>10</sup>J. van der Veen, W. H. de Jeu, M. W. M. Wanninkhof, and C. A. M. Tienhoven, *J. Phys. Chem.* **77**, 2153 (1973).
- <sup>11</sup>We wish to thank Dr. H. van Sprang (Philips Research Laboratories, Eindhoven) for providing us with the *p*-xylylene coated glass plates.
- <sup>12</sup>W. H. de Jeu and W. A. P. Claassen, *J. Chem. Phys.* **68**, 102 (1978).
- <sup>13</sup>W. H. de Jeu and W. A. P. Claassen, *J. Chem. Phys.* **67**, 3705 (1977).
- <sup>14</sup>(a) A. F. Martins and A. C. Diogo, *Port. Phys.* **9**, 129 (1975); (b) J. Prost, G. Sigaud, and B. Regaya, *J. Phys. Lett.* **37**, L-341 (1976); (c) G. Marrucci, *Mol. Cryst. Liq. Cryst. Lett.* **72**, 153 (1982); (d) A. C. Diogo and A. F. Martins, *J. Phys.* **43**, 779 (1982).